Engineering Failure Analysis 158 (2024) 108050

Contents lists available at ScienceDirect

Engineering Failure Analysis

journal homepage: www.elsevier.com/locate/engfailanal

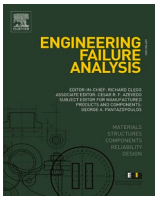

Mechanical evaluation analysis of pipe-liner composite structure before and after polymer grouting rehabilitation

Kangjian Yang [a,b,c], Hongyuan Fang [a,b,c,d,*], Xijun Zhang [a,b,c], Xueming Du [a,b,c,*], Bin Li [a,b,c], Kejie Zhai [a,b,c]

[a] Yellow River Laboratory, Zhengzhou University, Zhengzhou 450001, China
[b] National Local Joint Engineering Laboratory of Major Infrastructure Testing and Rehabilitation Technology, Zhengzhou 450001, China
[c] Collaborative Innovation Center of Water Conservancy and Transportation Infrastructure Safety, Henan Province, Zhengzhou 450001, China
[d] Southern Engineering Inspection and Restoration Technology Research Institute, Huizhou 516029, China

ARTICLE INFO

Keywords:
Concrete pipe
Surrounding void
CIPP rehabilitation
Polymer grouting
Pipe joint
Mechanical performances

ABSTRACT

In practical engineering, voids can still be present in pipelines even after cured-in-place pipe (CIPP) rehabilitation, which requires polymer grouting for repair. However, the effectiveness of polymer grouting is uncertain. To solve this engineering problem, a series of full-scale tests were conducted to analyze the mechanical differences of the pipe-liner structure before and after polymer grouting. Subsequently, a three-dimensional numerical model was established to supplement the limited full-scale test data, and the evaluation indices of mechanical properties of pipe joints, such as shear displacement, relative rotation, and bending moment, were analyzed. Finally, 20 sets of comparison experiments (containing different loading and voiding cases) were designed and statistically analyzed to evaluate the repair effect of polymer grouting. The results show that polymer grouting has a significant impact on the mechanical properties of the pipe-liner structure, effectively preventing accidents such as gasket fall off and pipe disconnections by reducing the shear displacement and relative rotation of the pipe by 39.4 % and 43.6 %, respectively. Polymer grouting can change the stress state of the pipe, with the average bending moments at the crown and springline of the pipe and the bending moment of the CIPP liner decreasing by 21.2 %, 12.0 % and 83.7 %, respectively, while increasing by 75.4 % at the invert of the pipe after the polymer grouting. When voids around the pipeline are found in practical engineering, polymer grouting should be used in a timely manner for repair.

1. Introduction

Underground pipelines play a crucial role in cities as they are responsible for energy transportation, information transmission, drainage, and water supply [1]. As of 2021, the total length of underground pipelines in China has exceeded 3.45 million kilometers, with approximately 40 % of the total pipeline length built before 2012 [2]. However, the long-term loading of pipelines can lead to various problems, such as corrosion, cracks, and voids [3,4]. Irregular management and delayed rehabilitation can exacerbate these issues, ultimately leading to pipeline leakage, environmental pollution, and even road collapse [5,6]. Accidents resulting from pipeline failures have caused significant losses to the national economy and raised widespread concern in society [7]. Therefore, it is essential to

* Corresponding authors at: Yellow River Laboratory, Zhengzhou University, Zhengzhou 450001, China.
E-mail addresses: 18337192244@163.com (H. Fang), 2007-dxm@163.com (X. Du).

https://doi.org/10.1016/j.engfailanal.2024.108050
Received 1 November 2023; Received in revised form 9 January 2024; Accepted 25 January 2024
Available online 1 February 2024

develop effective strategies for pipeline maintenance and rehabilitation to ensure the safety and sustainability of urban infrastructure.

In current engineering practice, two methods are used to solve pipeline problems: excavation-based rehabilitation and trenchless rehabilitation [8]. However, excavation-based methods have several disadvantages, including traffic disruptions, lengthy construction periods, and environmental pollution. Therefore, these methods are no longer feasible for underground pipeline maintenance in large cities [9,10]. Recently, pipeline trenchless rehabilitation technologies have been successfully employed, which mainly includes internal and external pipeline rehabilitation techniques, such as sliplining, pipe bursting, CIPP lining, polymer grouting, cement grouting, and soil reinforcement [10]. Among the internal rehabilitation techniques, CIPP is widely used because of its advantages, such as no grouting, fast construction speed, and low environmental impact [11]. Kaushal et al. [12] compared the social cost of CIPP rehabilitation and excavation pipeline replacement methods and found that CIPP rehabilitation had significantly lower social costs. Matthews et al. [13,14] presented case studies of CIPP rehabilitation and found that it had less impact on the environment and improved the structural performance of the pipeline. Some scholars have also investigated the effectiveness and performance of CIPP rehabilitation methods, as well as the factors that can affect their performance. Adebola et al. [15] used optical fibers to investigate the performance of pressure pipe liners spanning across a ring fracture, while Michael et al. [16] developed a numerical model to analyze the effect of circular wall loss on CIPP liner performances. Shou et al. [17] evaluated the effectiveness of CIPP rehabilitation considering different factors, such as surface loading conditions and liner deformability. Argyrou et al. [18] analyzed the performance of CIPP liners under seismic actions using a fracture test, and Fang et al. [19] determined the influence of internal defects and basic pipe loads (e.g., earth, traffic, and fluid loads) on the mechanical behavior of the pipeline and CIPP liner. Lastly, Yang et al. [20] performed a series of sensitivity analysis to identify the factors affecting the performance of pipelines and CIPP liners. This collection of studies contributes to a growing body of research on the development and implementation of trenchless pipeline rehabilitation technologies, with a focus on the use of CIPP.

CIPP is widely used in pipeline systems, but the current management mindset of rehabilitation focuses more on the rehabilitation of internal pipeline defects and neglects the rehabilitation of external pipeline defects [21]. Due to construction reasons, erosion and uneven settlement of the foundation, void and uncompacted conditions are common at the bottom of the pipe [22]. After the CIPP rehabilitation, the void and uncompacted conditions still existed at the bottom of the pipeline, which severely affect the service life of the pipeline [23]. Therefore, developing pretreatment technologies for external defects is very crucial to repair of pipelines with both internal and external defects [24]. Polymer grouting technology has the advantages of low cost, fast repair speed, small impact on the environment, and no shrinkage after repair, thus gaining increasing popularity recently [25]. The basic principle of the polymer grouting technology (Fig. 1) involves injecting two-component polymer materials into the cracks of the rock or soil [26]. When the two component materials are in contact with each other, they chemically react and their volume expands rapidly, achieving the effect of filling the cracks, strengthening the surrounding rock, and preventing seepage and leakage [27].

The mechanical performance of pipe-liner structures with void defects before and after polymer grouting is not well understood, and it is unclear whether external rehabilitation is necessary for pipelines after CIPP rehabilitation. To address this engineering issue, this study conducted a series of full-scale tests to monitor the strain state of the pipe-liner structure before and after polymer grouting. To complement the limited data from the full-scale tests, a 3D numerical model was established based on these tests. Focusing on the pipe joint, which is the most critical location of the pipeline, the study analyzed the shear displacement, relative rotation, and bending moment at the joint before and after polymer grouting. To evaluate the repair effect of polymer grouting, 20 comparative experiments were designed based on the numerical model, and the effectiveness of the polymer grouting was verified. This study's results offer valuable insights into the effectiveness of polymer grouting in pipeline rehabilitation and can help improve pipeline safety and durability.

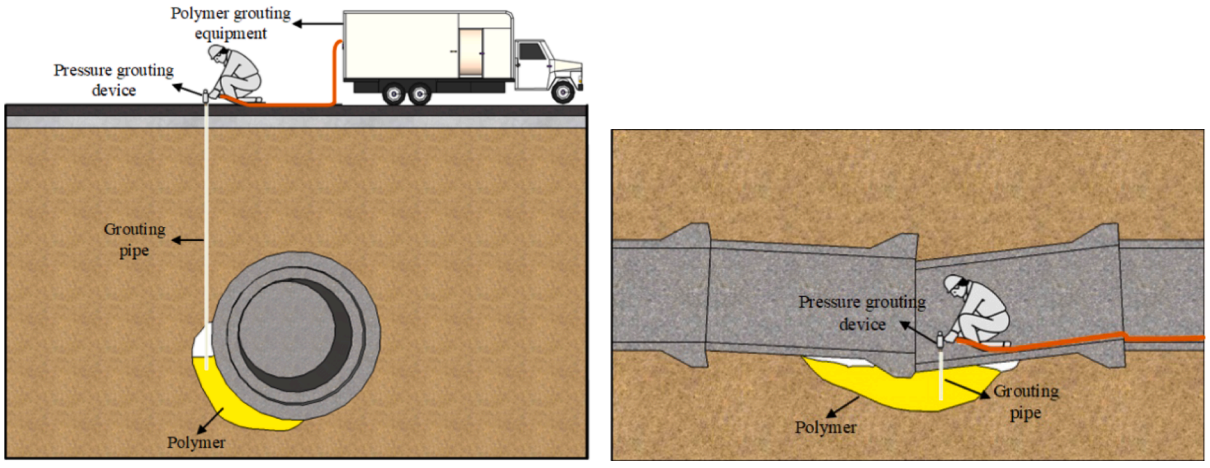

Fig. 1. Polymer grouting from the (a) inside (b) outside the pipe.

2. Full-scale tests

In this test, the construction process of the pipeline was performed according to the construction and acceptance of water and sewerage pipeline works (GB50268-2008) [28]. The construction process mainly includes: excavation of the pit, laying of sand bedding, installation of the pipeline, and backfilling of the soil. The longitudinal section of this test is shown in Fig. 2. The material parameters of the soil, sand bedding and polymer in the full-scale test were determined by field sampling, where density was determined by the cutting ring method, modulus of elasticity by uniaxial compression test, Poisson's ratio was converted by the coefficient of static lateral pressure, and the angle of internal friction and cohesion were determined by the straight shear test. The material parameters of the pipe and CIPP liner were provided by the manufacturer. The material parameters for the full-scale test are shown in Table 1.

2.1. Pipeline defect configuration

2.1.1. Defective pipes

In practical engineering, the presence of defects such as corrosion and cracks inside pipes can significantly reduce their wall thickness, posing a serious risk to their safe operation. Qualit et al. [29] investigated the condition of drainage pipes in Rennes and found that defects were most common at the crown and invert, particularly at the crown, and less common at other locations. To investigate the effect of such defects, the defects in this study were intentionally placed at the crown and invert of the pipe, as illustrated in Fig. 3.

2.1.2. Void setting

Voids are a common problem in pipeline foundations. They cause uneven pipeline settlement and pipeline leakage. If not repaired in time, they can induce the formation of large cavities, leading to road collapse. In order to study the influence of voids on the structural performance of the pipe, a void located at J2 was established in this test, as shown in Fig. 4. The depth (d_i), length (l_i), and angle (α_i) of the void were set to 1 m, 0.2 m, and 150°, respectively.

2.2. Test equipment

2.2.1. CIPP rehabilitation

The ultraviolet (UV)-CIPP process involves inserting a thermoset resin-impregnated liner inside a defected underground pipeline, expanding the liner using inflatable equipment and curing the liner in place using UV light. The curing process of CIPP is shown in Fig. 5. In this test, the original pipe has not lost its bearing capacity and can bear most of the external loads. Thus, the CIPP thickness was determined based on partially deteriorated gravity pipe condition in ASTM F1216 [30], as shown below:

$$\mathrm{P} = \frac{2KE_L}{(1-\upsilon^2)}\cdot\frac{1}{(DR-1)^3}\cdot\frac{C}{N} \tag{1}$$

Where P is the groundwater load; $DR = \frac{D_0}{t}$ is the dimension ratio of CIPP liner; E_L is the elastic modulus of the CIPP; υ is the Poisson's ratio, K is the enhancement factor; C is the ovality reduction factor, and N is the safety factor.

2.2.2. Polymer grouting

In this test, the mass of each grouting is 125 g and the volume of grouting is 0.3768 m^3. Therefore, the density of polymer can be perfectly controlled by controlling the times of grouting. The method of polymer grouting outside the pipe was used to repair the void in this test. The grouting bag was preset (as shown in the Fig. 6(a)), and the polymer was injected into the grouting bag via the grouting pipe to eliminate the void (Fig. 6(b)).

2.2.3. Strain data collection equipment

The strain data were collected in this test, and the strain collection equipment consisted of three parts: strain gauges, strain data collection equipment and strain data analysis software. The strain gauges used in the system were BQ-80AA-P120 models, which have

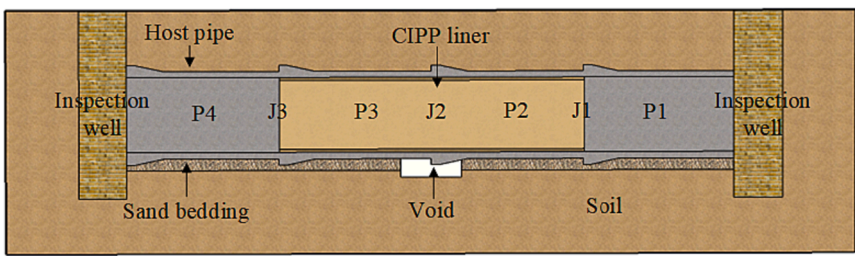

Fig. 2. Longitudinal section of the full-scale test.

Table 1
Material parameters.

Material	Density (kg.m^{-3})	Elastic modulus (MPa)	Poisson's ratio	Cohesion (KPa)	Angle of internal friction (°)
Soil	1613	30.1	0.25	9.3	21.2
Sand bedding	1872	52.7	0.2	1.6	35.4
Pipeline	2300	30,000	0.2	–	–
CIPP liner	1600	8800	0.3	–	–
Polymer	240	20	0.2	–	–

Fig. 3. The defected pipe.

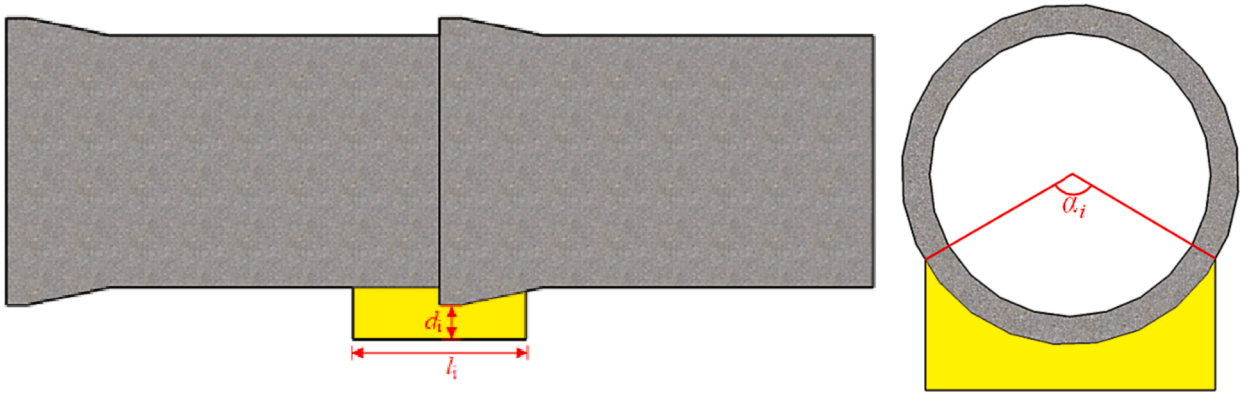

Fig. 4. The void of pipeline.

a resistance value of 120 Ω, an accuracy of 0.1 με, and a sensitivity coefficient of 2.2 %. The strain gauges were installed in a circumferential pattern ("✳") outside the P2 bell, P2 barrel, and P3 spigot on the pipeline, and in a longitudinal and circumferential pattern ("✳")inside the J2 and P2 barrel on the CIPP liner, as shown in Fig. 7. In order to eliminate the effect of temperature on strain during the full-scale test, the bridge circuit with temperature compensation was employed in this test, which consists of the following steps: 1) The temperature-compensated strain gauges are attached to the temperature-compensated specimen, where the material properties of the temperature-compensated specimen are the same as those of the test specimen; 2) Connect the temperature-compensated strain gauges to the temperature-compensated channel of the DH3816N; 3) Place the temperature-compensated specimen in the same temperature field as the test specimen and ensure that the temperature-compensated specimen is not subjected to any

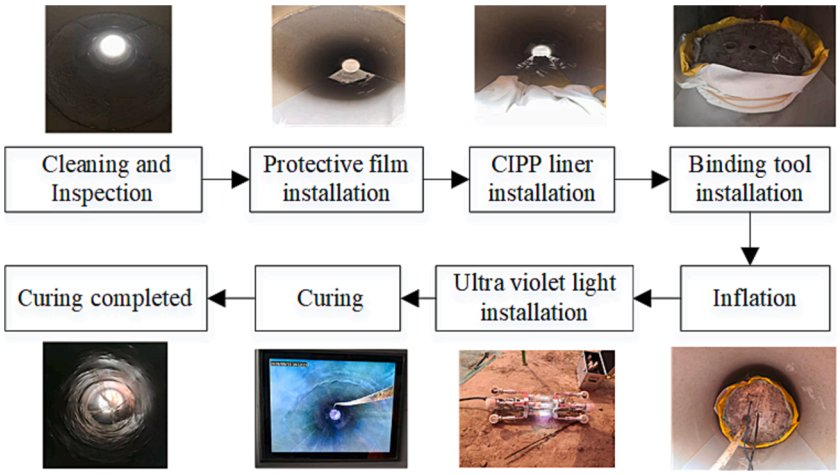

Fig. 5. The curing process of CIPP.

Fig. 6. (a) Preset of grouting bag (b) Effect of polymer grouting rehabilitation.

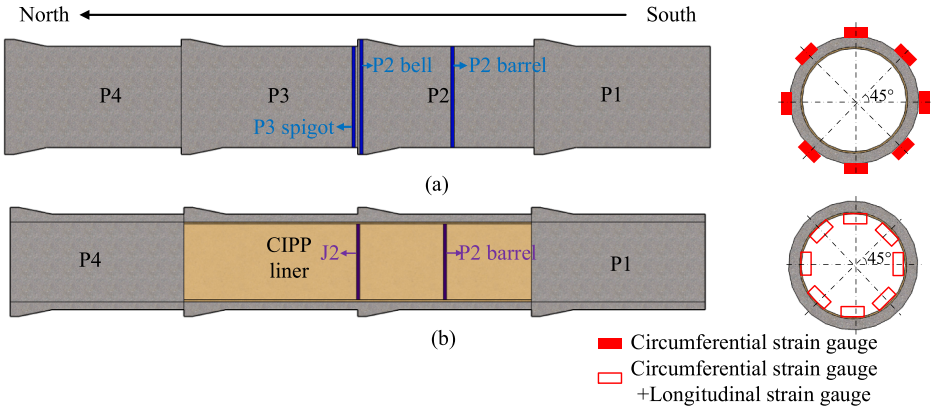

Fig. 7. Installation of strain gauges.

external loads.

2.3. Test methods

The testing procedure for this study involved four main steps:

(1) Connecting and activating the strain data collection equipment.
(2) Importing the zero point data of the pipe into the data collection equipment and placing a truck of specified weight at J2 of the pipe.
(3) Initiating the strain data collection process using the equipment at a frequency of 2 Hz.
(4) Terminating the strain collection process when stable data had been recorded.

2.4. Test results

The impact of polymer grouting on the repair of pipe-liner composite structures is not well understood. To address this engineering issue, the strains of the composite structures before and after polymer grouting were extracted and analyzed, as illustrated in Fig. 8 and Fig. 9.

In Fig. 8, the pipe exhibits negative values of circumferential strain at the crown and invert and positive values at the springline, revealing that the crown and invert experience compression, while the springline experiences tension. Near the void area, the strain is close to zero because the soil provides almost no support to the pipe due to the presence of the void. After polymer grouting, the circumferential strain at the crown and springline of the pipe bell is reduced by 29.8 % and 14.9 %, respectively, and increased by 298.2 % at the pipe invert. Similarly, the circumferential strain at the crown and springline of the pipe spigot is reduced by 27.6 % and 15.3 %, respectively, and increased by 285.7 % at the pipe springline. By comparing the circumferential strains of the pipe before and after the polymer grouting rehabilitation, it is evident that the polymer grouting can improve the stress state of the pipe and make it more reasonable.

Fig. 9 shows that the CIPP liner is under tension at the crown and invert and compression at the springline in the circumferential direction; while the CIPP liner experiences compression at the crown and tension at the springline and invert in the longitudinal direction. After the polymer grouting rehabilitation, the strains at the crown, springline, and invert of the CIPP liner decreased by 23.6 %, 14.6 %, and 21.7 %, respectively, in the circumferential direction, and 61.2 %, 20.3 %, and 70.8 % in the longitudinal direction. Comparative analysis reveals that the strain reduction in the longitudinal direction of the CIPP liner is greater than that in the circumferential direction. This phenomenon can be attributed to the uneven force acting on the pipe bell-spigot structure, causing shear displacement and rotation at the pipe joints, which leads to a significant increase in tensile stress of the CIPP liner in the longitudinal direction. Moreover, the situation is exacerbated in the presence of void at the bottom of the pipe. Therefore, repairing the void can effectively reduce the stress in the longitudinal direction of the CIPP liner.

From the above analysis, it can be found that the polymer grouting rehabilitation can reduce and improve the stress state and extend the service life of the pipe-liner composite structure.

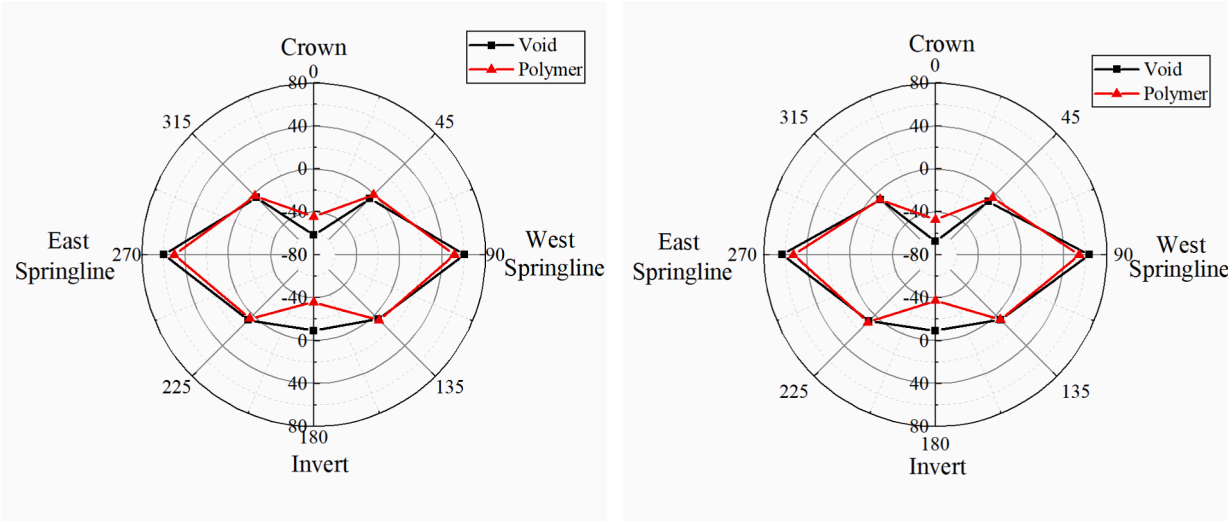

Fig. 8. Circumferential strain of (a) spigot and (b) bell of pipe before and after polymer grouting rehabilitation.

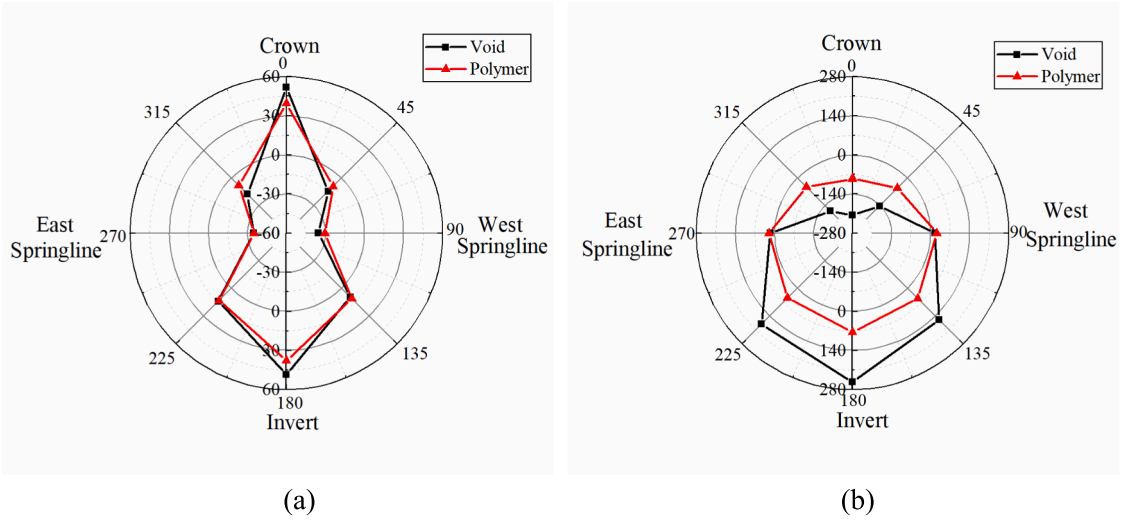

Fig. 9. (a) Circumferential strain and (b) longitudinal strain of CIPP liner at the pipe joint before and after polymer grouting rehabilitation.

3. Numerical simulation tests

3.1. Establishing numerical model

In this study, it was challenging to obtain sufficient data for comparative analysis due to the limited acquisition of data from the full-scale test. The research findings demonstrated that the asymmetry of the bell-spigot structure's geometric shape and uneven soil settlement lead to rotation and shear displacement of the pipeline structure at the pipe joints, which can pose a significant risk of pipeline leakage and endanger the pipeline's safe operation. However, acquiring rotation and shear displacement data from full-scale tests is difficult. To overcome this challenge, a series of numerical simulations were conducted based on the full-scale test.

3.1.1. Model description

In this study, a three dimensional (3-D) numerical simulation model was developed to investigate the pipe-liner composite structure's behavior. The simulation model consisted of five parts, including the pipeline, CIPP liner, soil, polymer, and gaskets, as illustrated in Fig. 10(a). The numerical simulation model's dimensions were 10 m (length) × 10 m (width) × 8 m (height), and it included four sections of pipes. The geometry of pipe was selected according to the concrete and reinforced concrete sewer pipes (GB/T 11836-2009) [31], as shown in Fig. 10(b). The CIPP liner was modeled using a linear elasticity model, while the Drucker-Prager constitutive model and a concrete damaged plasticity (CDP) model were selected for the soil and pipelines, respectively [32]. The setting parameters of CDP model are shown in Table 2 and the compression and tensile stress–strain curve of CDP is shown in Fig. 11. The Mooney–Rivlin strain energy function was chosen as the material model for the gaskets. All components included in the model are deformable solid parts, and it is assumed that all components have homogeneous properties when assigning material properties to them. The material parameters are consistent with the parameters of the full-scale test, as shown in Table 1.

3.1.2. Model steps

The analytical step of the numerical simulation model consists of 3 main sections, as follows:

(1) Creating a "geostatic step" to obtain the initial geostatic stress of the soil.
(2) Setting the predefined field of the soil based on the numerical results calculated in step.
(3) Creating a "static general step" to obtain the results of the calculations under coupled traffic and soil loads.

3.1.3. Model interfaces

The interfaces in the numerical simulation model comprised five parts: soil–pipe, pipe–liner, pipe–gasket, polymer–soil, and polymer–pipe interfaces. The normal and tangential directions of the interface between the soil and the pipe are "*hard*" and "*penalty*", respectively. The tangential friction coefficient of tangential direction was determined using Equation (2) [33]:

$$\mu = \frac{A}{H/D - B} + C \tag{2}$$

where H is the cover depth; D is the diameter of the pipeline; and A, B, and C are the fitting parameters.

After the CIPP rehabilitation process, an adhesive bond develops between the pipe and the CIPP liner. In this study, the isotropic Coulomb friction model was selected to simulate this bond [16].

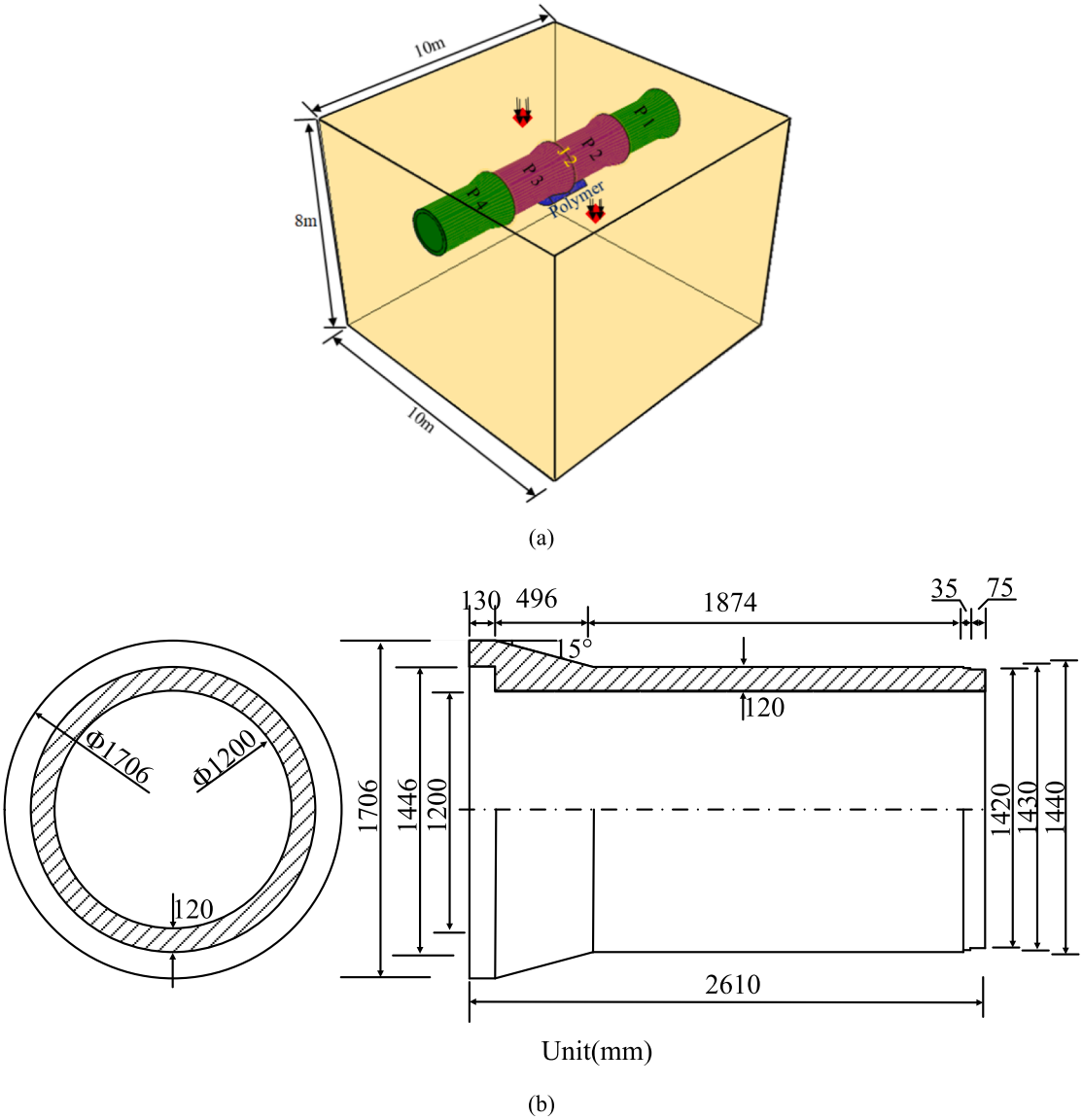

Fig. 10. (a) 3-D numerical simulation model and (b) Geometry of pipe joint.

Table 2
Material parameters of CDP.

Dilation Angle	Eccentricity	f_{b0}/f_{c0}	κ	Viscosity parameter
30	0.1	1.16	0.6667	0.005

In practical engineering, separation and slippage often occur between gaskets and pipes at pipe joints. To simulate this phenomenon, the interface between the pipe and gasket was established in this study. The interface parameters were set with reference to the study of Xu et al [34]. The normal stiffness of the interface was set to 10,000 GPa/m, the friction angle was set to 5°, and the shear stiffness was set to 8,000 GPa/m.

The polymer material undergoes large expansion and exhibits cohesiveness after grouting, forming a composite component with the surrounding medium to resist external loads. Therefore, a *tie* was applied to the polymer-soil and polymer-pipe interfaces.

3.1.4. Model load

The model loads in this study consist of two main components, soil loads and traffic loads. The soil load was applied in the "gravity" mode in the geostatic analysis step, where the gravity acceleration is 9.8 N/m^2. In the structural design of pipelines, traffic load is

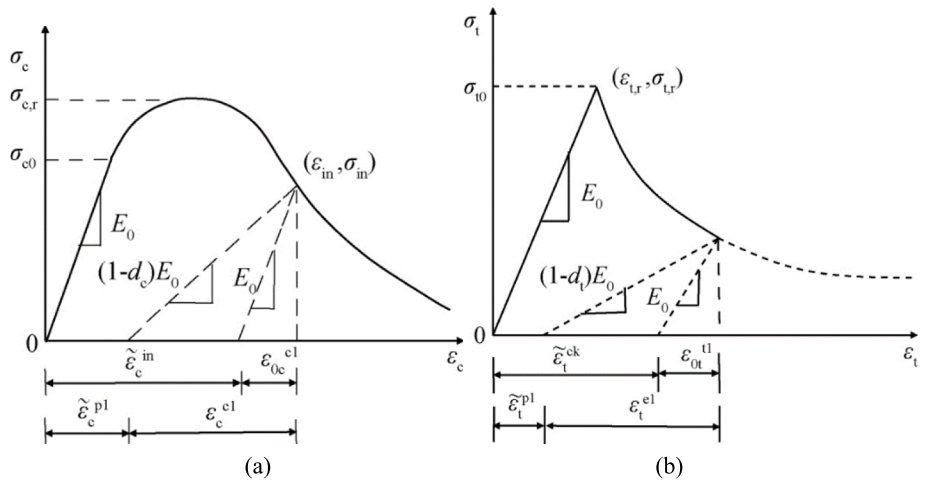

Fig. 11. Uniaxial (a) compression and (b) tensile stress–strain curve of CDP.

typically considered as a static load. In this study, the traffic loads are applied in the static generic analysis step in the form of "pressure", in which the traffic loads were applied on both sides of J2, with a wheel distance of 2.4 m and an area of 0.21 m × 0.21 m.

3.1.5. Meshing of numerical simulation model

The models adopted herein were meshed in Hypermesh, considering that meshing a 3D numerical model with a bell-and-spigot structure is difficult. The element of the model was meshed according to the Abaqus user manual to improve the accuracy of the

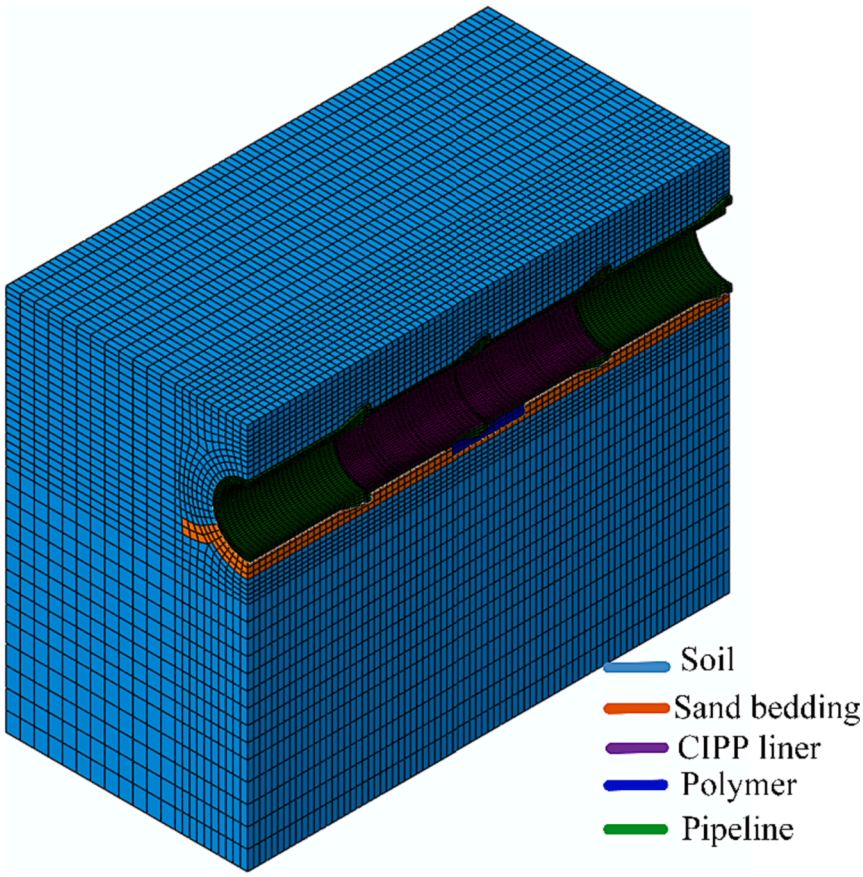

Fig. 12. Mesh geometry.

model. The mesh size of the model ranged between 0.02 and 0.2 m. The element of the pipeline was densely meshed in the corrosion area to obtain the accurate stress state of the corrosion area; the elements of the pipeline and the gasket were consistent in the circumferential direction to improve the contact quality of the pipeline and the gasket; The elements of the soil is dense in the area close to the pipeline and sparse in the area far from the pipeline to improve the computational efficiency of the model. The element type of the numerical simulation model was set as C3D8R in this study, and the hourglass control was enhanced. The mesh geometry is shown in Fig. 12.

3.2. Comparison of numerical results and full-scale test results

To evaluate the accuracy and stability of the numerical simulation model, the simulated data from the model were compared and analyzed with the test data from the full-scale test, as presented in Figs. 13 and 14. In comparative analysis, the setting conditions and parameters of the 3D numerical model are constant with the full-scale tests. To assess the relative error between the full-scale test data and the numerical simulation data, the MAPE and RMSE were calculated. The equations used to calculate these values are shown below [35]:

$$MAPE = \frac{100\%}{n}\sum_{t=1}^{n}\left|\frac{A-F}{A}\right| \tag{3}$$

$$RMSE = \sqrt{\frac{1}{n}\sum_{t=1}^{n}(A-F)^2} \tag{4}$$

Where A is value of full-scale test data, F is value of simulated data and n is the sample size.

The results presented in Figs. 13 and 14 indicate that the simulated data and the test data exhibit consistent numerical magnitudes and distributions, with MAPE and RMSE values of 10.17 % and 6.97 for the simulated data, respectively. The calculation results of MAPE show that there is a small difference between the data of the numerical model established in this study and the full-scale tests, with an error range of about 10 %. Based on the comparative analysis, it can be concluded that the numerical simulation model is accurate and stable, and can be relied upon for further analysis.

3.3. Numerical test results

Pipe joints are susceptible locations for pipeline damage. Factors such as irregular construction, uneven pipeline foundation, long-term loading, and sudden natural disasters can cause rotation and shear displacement at the joints, which pose risks to the pipeline's safe operation. In the presence of voids, larger rotations occur at the pipe joints, dramatically increasing the risk of pipeline operation [36]. Therefore, vertical displacement and stress clouds of P2, P3, and CIPP liner were extracted to analyze the effect of polymer grouting on the safety of the pipeline system, as shown in Fig. 15, where the magnification factor of pipe deformation in the stress cloud is 1000 times.

As can be seen from Fig. 15, the vertical displacement of the pipe is greatly reduced after polymer grouting, and the rotation of the pipe is also greatly reduced accordingly. Due to the reduction of pipe rotation and vertical displacement, the longitudinal tensile stress of CIPP liner at the pipe joints is reduced and the von Mises stress of CIPP liner at the pipe joints is significantly reduced after polymer

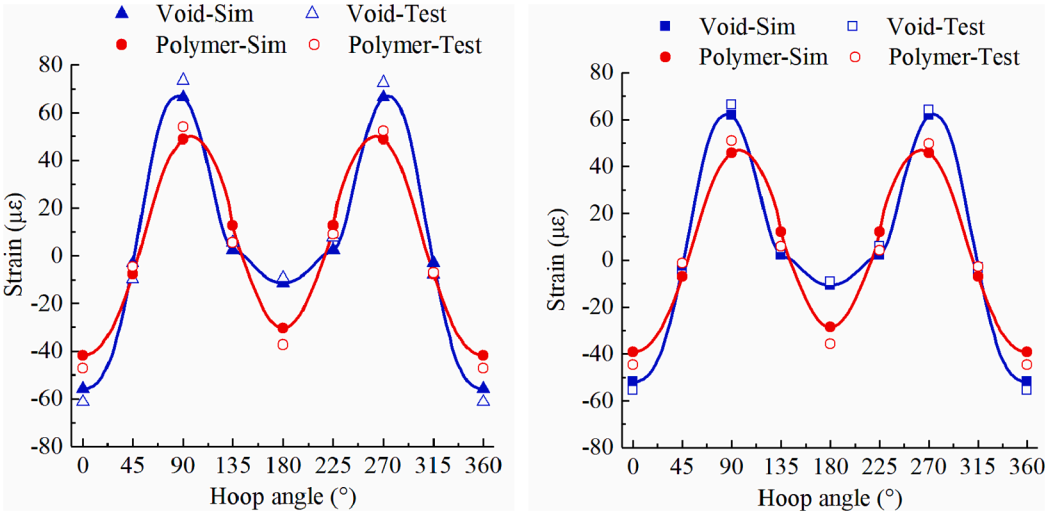

Fig. 13. Comparative analysis of circumferential strain data of (a) pipe spigot and (b) pipe bell.

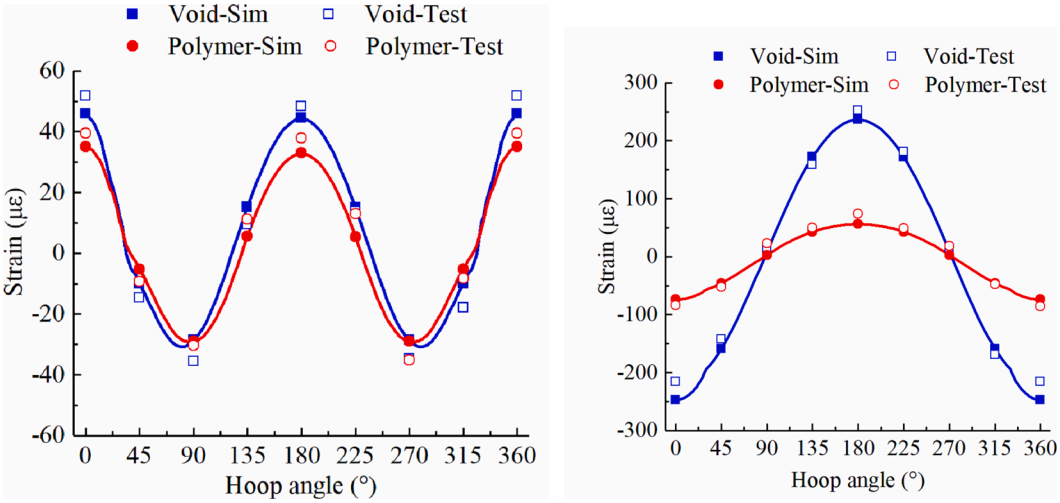

Fig. 14. Comparative analysis of (a) circumferential strain data and (b) longitudinal strain data of CIPP.

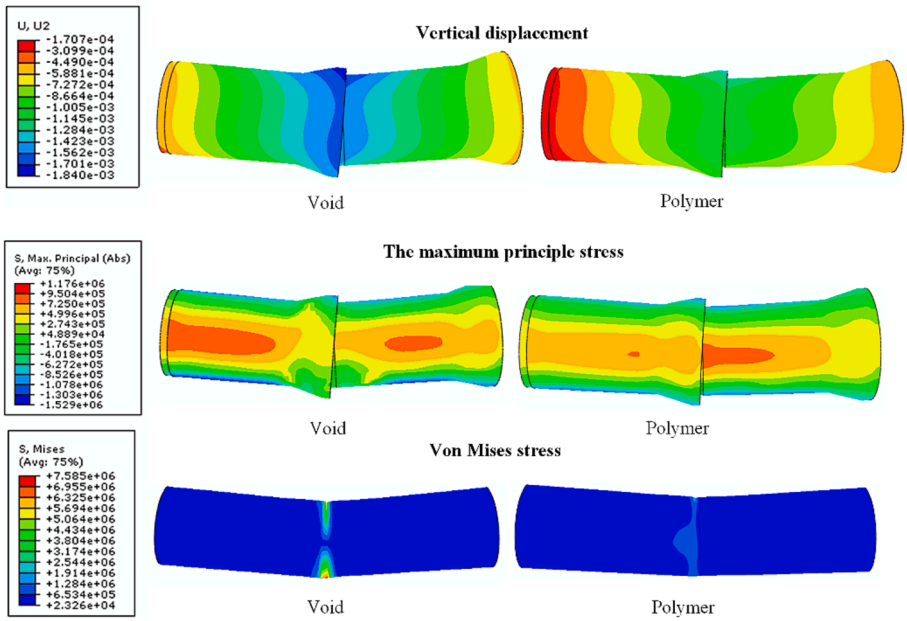

Fig. 15. Stress cloud of pipe-liner composite structure.

grouting. Before the polymer grouting rehabilitation, the presence of void at the pipe joints led to a lower stress concentration in the pipe joints. After the void was filled by the polymer, the stresses in the pipe were redistributed, resulting in increased stresses at the pipe joints and decreased stresses in the pipe barrel. From Fig. 15, it is evident that polymer grouting has a significant impact on the

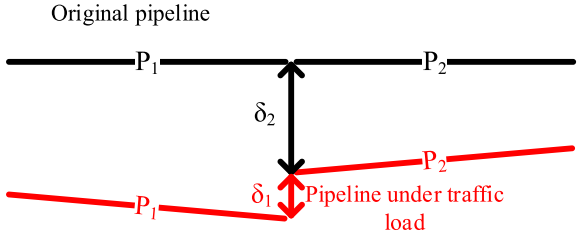

Fig. 16. Shear displacement of the pipe.

mechanical properties of the pipe and CIPP liner.

To quantify the impact of polymer grouting, displacement, strain, and stress data of the composite structure were extracted for further analysis. Additionally, shear displacement and relative rotation of the pipe, which are not easily obtained in field experiments, were extracted through simulation tests. A comparative analysis was subsequently performed to assess the effect of polymer grouting on the performance of pipe joints.

3.3.1. Shear displacement of the pipe before and after polymer grouting

The shear displacement is defined as the vertical displacement difference between two adjacent pipes at the pipe joints, as shown in Fig. 16. Due to the asymmetric geometry of the pipe bell and pipe spigot, the vertical displacement curve of the pipeline exhibits high discontinuity at the pipe joint under load, particularly under concentrated loads such as traffic loads and surcharge loads [37]. The shear displacement significantly affects the mechanical behavior of the pipe-liner composite structure. Although the CIPP liner reduces the pipe shear displacement after rehabilitation, it also causes a sharp increase in stress in the CIPP liner, as it is a continuous pipe. To evaluate the effect of polymer grouting, numerical models were developed and analyzed under different traffic loads before and after polymer grouting, where the cover depth, void depth, void length, and void angle of 1 m, 20 cm, 1.5 m, and 90°, respectively. The calculation method for the shear displacement of pipe is shown in Equation (5) [25]. Fig. 17 illustrates the obtained results.

$$\delta = V_1 - V_2 \tag{5}$$

Where δ is the shear displacement of the pipe at the pipe joint, V_1 is the vertical displacement of P_1 at the pipe joint, and V_2 is the vertical displacement of P_2 at the pipe joint.

As shown in Fig. 17, it is evident that the shear displacement of the pipe increases linearly with an increase in traffic load, indicating a significant influence of traffic load on the shear displacement of the pipe. However, after polymer grouting rehabilitation, the shear displacement of the pipe decreased by 39.4 %. This reduction is attributed to the filling of the void beneath the pipe with polymer, which, in turn, decreased the vertical displacement of the pipe and significantly reduced its shear displacement under the same load. Thus, it can be inferred from Fig. 17 that polymer grouting can effectively mitigate the shear displacement of the pipe, consequently enhancing the safety of the pipe structure.

3.3.2. Relative rotation of the pipe before and after polymer grouting

The relative rotation refers to the angle between the pipe axes of two adjacent pipes, as depicted in Fig. 18. Due to the unevenness of the pipeline foundation and load, the relative rotation of the pipeline is a common occurrence. The impact of relative rotation on the safe operation of the pipeline structure mainly manifests in two aspects. Firstly, it can lead to functional failure of the pipeline, causing movement of the gasket and axial movement of the pipeline, which may result in the gasket falling off or the pipeline disconnecting. Secondly, it can cause structural failure of the pipe by squeezing the bell-spigot structure and leading to a sharp increase in the longitudinal strain of the CIPP liner, causing rupture of the bell-spigot structure [38]. In order to evaluate the repair effect of polymer grouting, the relative rotation of the pipe before and after polymer grouting rehabilitation was extracted, as shown in Fig. 19. The calculation method for the relative rotation of pipe is shown in Equation (6) [39].

$$\theta = \theta_1 + \theta_2 = \arcsin\frac{\Delta h_1}{L_0} + \arcsin\frac{\Delta h_2}{L_0} \tag{6}$$

Where Δh is the differences in vertical displacements at both ends of the pipe, and L_0 is the length of the pipe.

As shown in Fig. 19, the relative rotation of the pipeline increases linearly with the increase of traffic load, indicating a significant influence of traffic load on the relative rotation of the pipeline. After polymer grouting rehabilitation, the relative rotation of the pipeline decreased significantly by 43.6 %. This reduction can be attributed to the fact that the pipeline is more prone to rotate under traffic load, and the presence of void exacerbates this rotation. However, when the void is filled with polymer, the bottom of the pipeline is supported, thus limiting the rotation of the pipeline and significantly reducing its relative rotation.

3.3.3. Bending moment of the composite structure before and after polymer grouting

Bending moment is a kind of internal moment on the section of the stressed specimen, which is basically a force that causes something to bend in the most simple terms [40]. It represents the algebraic sum of all external forces acting on the section of the pipe to the centroid moment of the section. Studying the bending moment of the pipe cross-section is essential to identify the most critical cross-section of the pipe and evaluate its safety performance, making it a vital indicator of the pipe's mechanical properties [41]. The mechanical analysis of the pipe cross-section is depicted in Fig. 20. The bending moments of the pipeline and CIPP liner under different traffic loads are shown in Fig. 21 and Fig. 22.

From Fig. 20, the bending moment of the pipe can be calculated by the following equation [42]:

$$\sum M = M : \int_{d_{n2}}^{t} \sigma(x)xdx - \int_{0}^{d_{n2}} \sigma(x)xdx = M \tag{7}$$

It can be seen from Fig. 21 that the bending moment at the pipe bell is significantly greater than that at the pipe spigot, which is because the wall thickness at the pipe bell is thicker, and the bending moment is proportional to the square of the wall thickness. After the polymer grouting rehabilitation, the bending moments at the crown and springline of the pipe spigot decreased by 21.4 % and 12.3 %, respectively, while the bending moment at the invert of the pipe increased by 74.3 %. Similarly, the bending moments at the crown

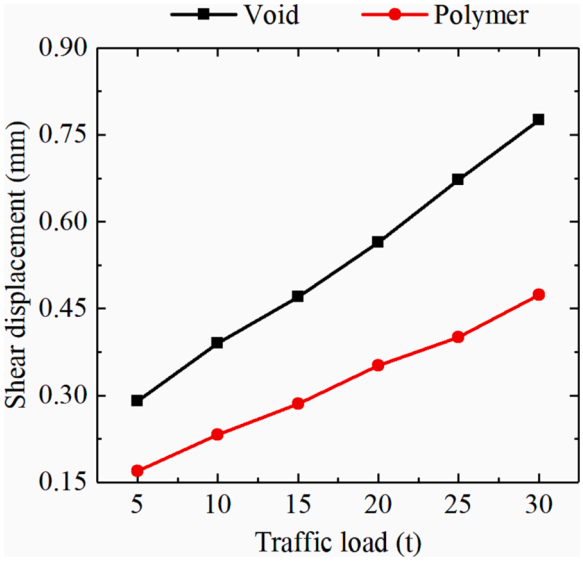

Fig. 17. Shear displacement of the pipe before and after polymer grouting.

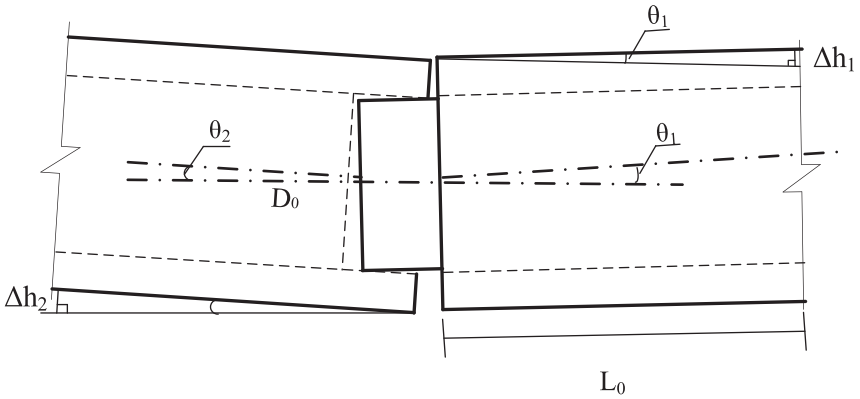

Fig. 18. Relative rotation of the pipe.

and springline of the pipe bell decreased by 20.9 % and 11.6 %, respectively, and increased by 76.4 % at the invert of the pipe. The increase of the bending moment at the invert of the pipe is due to the filling of the void at the bottom of the pipe by the polymer, which supports the bottom of the pipe, increases the interaction force between the pipe and the polymer, and significantly increases the bending moment at the invert of the pipe. Additionally, the decrease in the crown of the pipeline after polymer grouting is greater than that in the springline of the pipeline. This is because the load acts directly above the pipe joint, and there is no eccentric load, so the vertical rotation angle of the pipe is larger, and the horizontal rotation angle of the pipe is smaller, which causes the crown of the pipe to be squeezed larger, and the springline of the pipe squeeze less. Therefore, the bending moment at the crown of the pipe decreases greatly after the polymer grouting.

Fig. 22 illustrates that the bending moment of the CIPP liner decreases sharply to 83.7 % after polymer grouting rehabilitation. This can be attributed to the fact that the CIPP liner is a continuous pipe and its stress is highly susceptible to the rotation and shear displacement of the pipe. With the void being filled by the polymer, the rotation and shear displacement of the pipe reduce, resulting in a sharp decrease in the bending moment of the CIPP liner.

In light of the above analysis, it can be inferred that polymer grouting can reduce the vertical displacement and rotation angle of the pipeline, significantly decrease the bending moment of the CIPP liner, alter the stress state of the pipeline, and enhance the safety of the pipe-liner structure.

4. Discussion

To verify the effectiveness of polymer grouting and evaluate the repair effect, statistical analysis is essential. Due to the limited data from the full-scale tests and poor repeatability, simulation tests were conducted, and 20 sets of comparison experiments with different

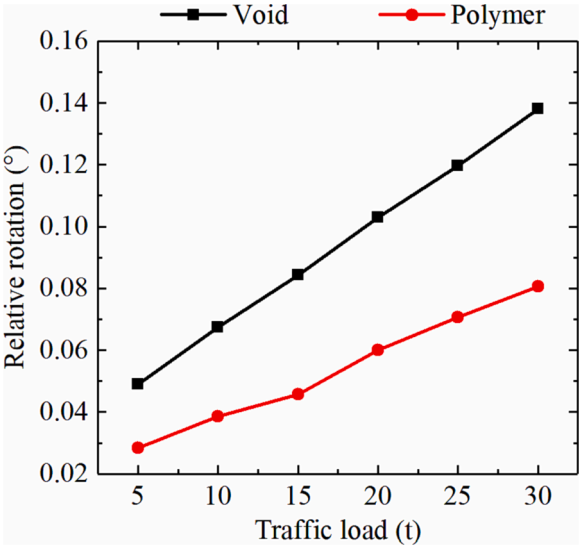

Fig. 19. Relative rotation of the pipe before and after polymer grouting.

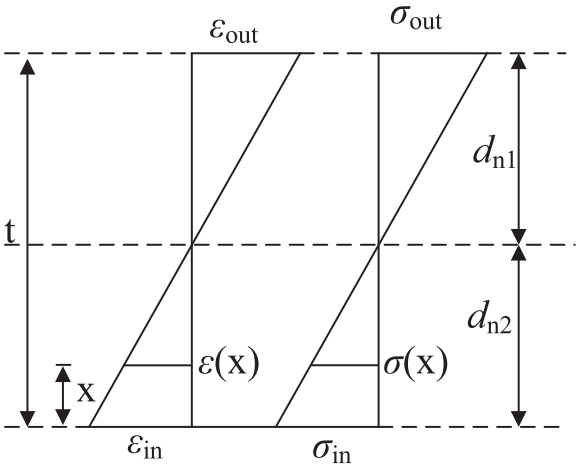

Fig. 20. Mechanical analysis of pipe cross-section.

loading and voiding cases were designed to analyze the differences in the mechanical properties of the pipe-liner structure before and after the polymer grouting, and the shear displacement, relative rotation, and bending moment were selected as evaluation indexes. The calculation results are presented in Table 3, where "SD" represents shear displacement, "RR" represents relative rotation, "BMP" represents bending moment of the pipe, and "BMC" represents bending moment of CIPP. The steps and principles of statistical analysis for each evaluation index are presented below [43]:

The calculated results of the evaluation indexes were noted as (X_1,Y_1),……(X_{20},Y_{20}). Assuming that each pair of data is independent of each other, the expressions of (X_i,Y_i) are:

$$(X_i, Y_i)\ N\left(\alpha_1+\beta_i, \alpha_2+\beta_i, \sigma_1^2, \sigma_2^2, \rho\right), i = 1, \cdots, n, \tag{8}$$

Where α_1, α_2 are the mean values before and after polymer grouting, respectively, and β_i is the effect of the i_{th} test condition. To determine whether the polymer grouting has a significant effect on the pipe-liner structure, then the test equation can be listed:

$$H_0 : \alpha_1 = \alpha_1; H_1 : \alpha_1 \neq \alpha_1 \tag{9}$$

In order to eliminate the effect of test conditions, let $Z_i = X_i\text{-}Y_i$, i = 1,2,…,n, then $Z_i \sim N(\mu, \sigma^2)$, where $\sigma^2 = \sigma_1^2 + \sigma_2^2 - 2\rho\sigma_1\sigma_2$. Then the test equation of the problem is:

$$H_0 : \mu = 0; H_1 : \mu \neq 0 \tag{10}$$

Therefore, the test statistic of this problem is:

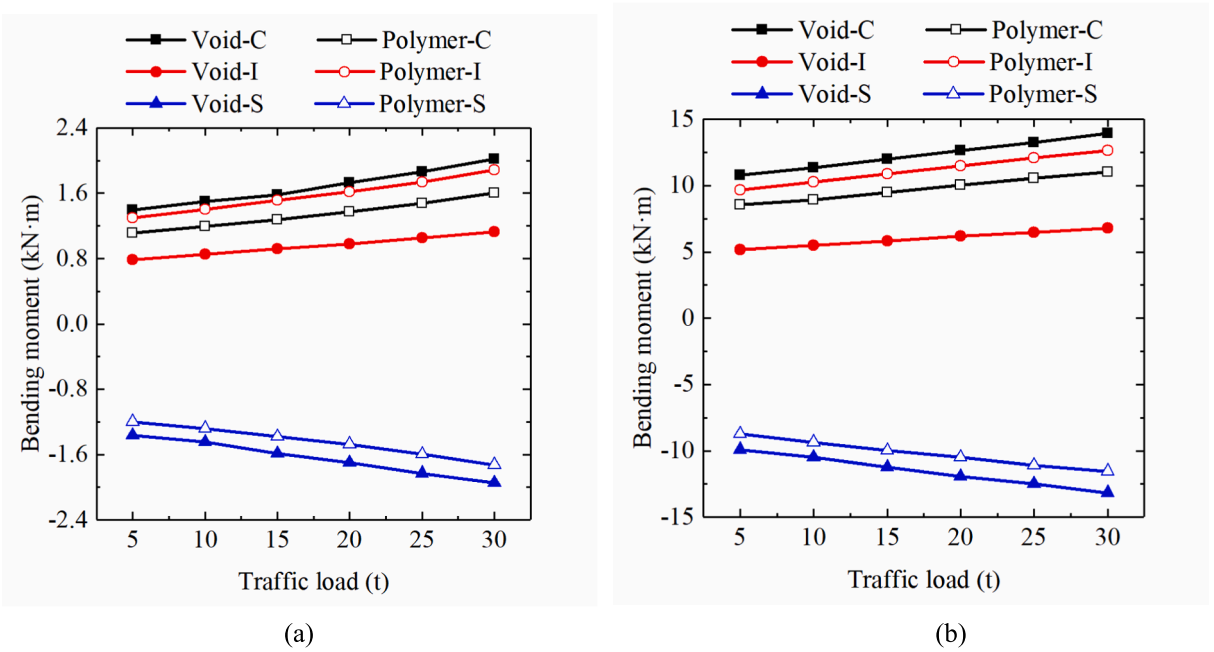

Fig. 21. Bending moment of the pipe (a) spigot and (b) bell before and after polymer grouting.

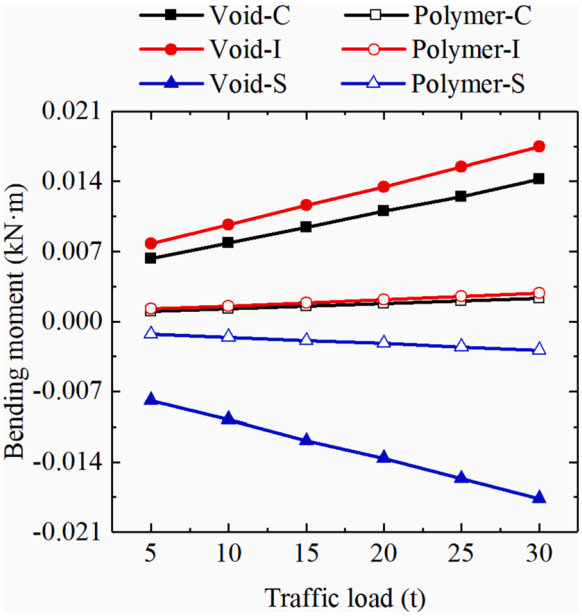

Fig. 22. Bending moment of the CIPP liner before and after polymer grouting.

$$T = \frac{\overline{Z}}{S/\sqrt{n}} \tag{11}$$

The calculated results of the statistics of each evaluation index are shown in Table 4.

Table 4 shows that all evaluation indexes of the pipe-liner structure fall within the confidence interval, indicating that there is a high probability of 99 % in rejecting H_0, and that the difference in evaluation indexes before and after polymer grouting is highly significant. Thus, based on the analysis conducted, it can be concluded that polymer grouting repair is effective, and it has a significant impact on the mechanical properties of the pipe-liner structure. This is because after polymer grouting, the polymer will fill the voids at the bottom of the pipe and increase the support for the pipe, which will reduce the vertical displacement of the pipe-liner structure. The

Table 3
Values of evaluation indexes of pipe-liner structure.

Void				Polymer			
SD(mm)	RR (°)	BMP (kN.m)	BMC (kN.m)	SD(mm)	RR (°)	BMP (kN.m)	BMC (kN.m)
0.2952	0.0494	10.7856	0.0078	0.1692	0.0284	9.6547	0.0013
0.3968	0.0675	11.3616	0.0097	0.2324	0.0386	10.25483	0.0016
0.4781	0.0843	12.0028	0.0116	0.2865	0.0457	10.86354	0.0019
0.5642	0.1034	12.6649	0.0134	0.3523	0.0635	11.4854	0.0022
0.6721	0.1196	13.2682	0.0154	0.4012	0.0707	12.07814	0.0025
0.7755	0.1382	13.9644	0.0175	0.4741	0.0807	12.63395	0.0028
0.5124	0.0991	11.727	0.0126	0.3467	0.0628	11.145	0.0021
0.5273	0.1006	11.948	0.0129	0.3484	0.0630	11.151	0.0021
0.5446	0.1022	12.307	0.0132	0.3477	0.0633	11.309	0.0022
0.5792	0.1046	13.024	0.0137	0.3515	0.0640	11.620	0.0023
0.5961	0.1060	13.382	0.0139	0.3549	0.0646	11.753	0.0023
0.4431	0.0875	11.474	0.0095	0.3592	0.0657	11.097	0.0028
0.4969	0.0921	11.952	0.0105	0.3577	0.0648	11.234	0.0026
0.5318	0.1054	12.407	0.0128	0.3551	0.0640	11.350	0.0025
0.5933	0.1105	12.852	0.0141	0.3484	0.0629	11.587	0.0023
0.6324	0.1151	13.039	0.0150	0.3458	0.0625	11.631	0.0020
0.4572	0.0906	11.6906	0.0103	0.3584	0.0647	11.2830	0.0023
0.5125	0.0988	12.0317	0.0119	0.3568	0.0641	11.3705	0.0021
0.6177	0.1086	12.9776	0.0145	0.3507	0.0631	11.6133	0.0021
0.6618	0.1158	13.6391	0.0163	0.3476	0.0628	11.7307	0.0020

Table 4
Calculated results of statistics of evaluation indexes.

Evaluation indexes	Mean value	Standard deviation	Confidence interval	t	freedom	Sig.
SD	0.2022	0.6618	(0.1598,0.2445)	13.661	19	0.000
RR	0.0390	0.1029	(0.0324,0.0456)	16.942	19	0.000
BMP	1.0826	0.3970	(0.8287,1.3367)	12.196	19	0.000
BMC	0.0106	0.0023	(0.0091,0.0121)	20.489	19	0.000

shear displacement and relative rotation of the pipe-liner structure are positively correlated with its vertical displacement, so the shear displacement and relative rotation of the pipe-liner structure will also decrease after polymer grouting. In addition, the polymer grouting will increase the interaction force between the pipe and the polymer, reduce the compression at the pipe joints, and make the stress state of the pipe-liner structure more reasonable, so the bending moment of the pipe-liner structure will also be reduced after the polymer grouting.

5. Conclusions

In this study, a comprehensive investigation was conducted on the effectiveness of polymer grouting for repairing voids in pipelines. Full-scale tests were performed, followed by the establishment of a three-dimensional numerical model to supplement the limited data obtained from the full-scale test. Evaluation indices for mechanical properties, such as shear displacement, relative rotation, and bending moment, were proposed and analyzed. To verify the effectiveness of polymer grouting, 20 sets of comparison experiments were designed and statistically analyzed. The main findings are shown as follows:

(1) Polymer grouting can effectively prevent accidents such as gasket fall off and pipe disconnections by reducing the shear displacement and relative rotation of the pipe by 39.4 % and 43.6 %, respectively. This ensures the operation safety of the pipeline.
(2) Polymer grouting can fill voids and change the stress state of the pipe. After the polymer grouting, the average bending moments at the crown and springline of the pipe decreased by 21.2 % and 12.0 %, respectively, while increasing by 75.4 % at the invert of the pipe.
(3) Polymer grouting can significantly reduce the stress in the CIPP liner. After the polymer grouting, the bending moment of the CIPP liner was reduced by 83.7 % due to stress of CIPP liner is very sensitive to the rotation and shear displacement and polymer grouting can significantly reduce rotation and shear displacements.
(4) After statistical analysis of 20 sets of comparative experiments, the effectiveness of polymer grouting is supported with a 99 % probability. Polymer grouting has a significant impact on the mechanical properties of the pipe-liner structure.

CRediT authorship contribution statement

Kangjian Yang: Conceptualization, Data curation, Investigation, Software, Writing – original draft, Writing – review & editing.

Hongyuan Fang: Funding acquisition, Project administration, Resources, Writing – review & editing. **Xijun Zhang:** Formal analysis, Software. **Xueming Du:** Methodology, Writing – review & editing. **Bin Li:** Data curation, Methodology. **Kejie Zhai:** Software, Validation.

Declaration of competing interest

The authors declare that they have no known competing financial interests or personal relationships that could have appeared to influence the work reported in this paper.

Data availability

Data will be made available on request.

Acknowledgments

This research was funded by the National Key Research and Development Program of China (No. 2022YFC3801000), the Key Specialized Research and Development Breakthrough in Henan Province (232102321073), the National Natural Science Foundation of China (No. 52309174), the Postdoctoral Innovation Talent Support Program of China (No. BX20230328), the National Natural Science Foundation of China (No. 52208375), the Postdoctoral Research Foundation of China (2022TQ0305, 2022M722884), the national Natural Science Foundation of China Project (No. 52178368), and the Youth Talent Promotion Project of Henan Province (2023HYTP016), for which the authors are grateful.

References

[1] I.D. Moore, J.R. Booker, Ground failure around buried tubes, Rock Mech. Rock Eng. 20 (4) (1987) 243–260, https://doi.org/10.1007/BF01024644.
[2] B. Li, F. Wang, H. Fang, K. Yang, X. Zhang, Y. Ji, Experimental and numerical study on polymer grouting pretreatment technology in void and corroded concrete pipes, Tunn. Undergr. Space Technol. 113 (2021) 103842, https://doi.org/10.1016/j.tust.2021.103842.
[3] S. Alam, R.L. Sterling, E. Allouche, W. Condit, J. Matthews, A. Selvakumar, J. Simicevic, A retrospective evaluation of the performance of liner systems used to rehabilitate municipal gravity sewers, Tunn. Undergr. Space Technol. 50 (2015) 451–464, https://doi.org/10.1016/j.tust.2015.08.011.
[4] K. Zhai, I. Moore, Axial stresses in pressure pipe liners spanning joints with initial gap, opening as a result of differential ground movements, Tunn. Undergr. Space Technol. 133 (2023) 104965, https://doi.org/10.1016/j.tust.2022.104965.
[5] Matthews, John, Gay, Leon, Das, Susen, Bayat, Alireza, Salimi, Mahmoud, A comprehensive review on the challenges of cured-in-place pipe (CIPP) installations, J. Water Supply: Res. Technol. 65 (8) (2016) 583-596, doi:10.2166/aqua.2016.119.
[6] K.J. Zhai, H.Y. Fang, B. Li, C.C. Guo, K.J. Yang, X.M. Du, M.R. Du, N.N. Wang, Failure experiment on CFRP-strengthened prestressed concrete cylinder pipe with broken wires, Tunn. Undergr. Space Technol. 135 (2023), https://doi.org/10.1016/j.tust.2023.105032.
[7] J. Wu, Y. Bai, W. Fang, R. Zhou, G. Reniers, N. Khakzad, An integrated quantitative risk assessment method for urban underground utility tunnels, Reliab. Eng. Syst. Saf. 213 (2021) 107792, https://doi.org/10.1016/j.ress.2021.107792.
[8] B. Li, W. Yu, Y. Xie, H. Fang, X. Du, N. Wang, K. Zhai, D. Wang, X. Chen, M. Du, M. Sun, X. Zhao, Trenchless rehabilitation of sewage pipelines from the perspective of the whole technology chain: A state-of-the-art review, Tunn. Undergr. Space Technol. 134 (2023) (2023) 105022, https://doi.org/10.1016/j.tust.2023.105022.
[9] D.N. Chapman, P.C.F. Ng, R. Karri, Research needs for on-line pipeline replacement techniques, Tunn. Undergr. Space Technol. 22 (5–6) (2007) 503–514, https://doi.org/10.1016/j.tust.2007.05.004.
[10] H. Zhu, T. Wang, Y. Wang, V.C. Li, Trenchless rehabilitation for concrete pipelines of water infrastructure: A review from the structural perspective, Cem. Concr. Compos. 123 (2021) 104193, https://doi.org/10.1016/j.cemconcomp.2021.104193.
[11] Y. Xia, M. Shi, C. Zhang, C. Wang, X. Sang, R. Liu, P. Zhao, G. An, H. Fang, Analysis of flexural failure mechanism of ultraviolet cured-in-place-pipe materials for buried pipelines rehabilitation based on curing temperature monitoring, Eng. Fail. Anal. 142 (2022) 106763, https://doi.org/10.1016/j.engfailanal.2022.106763.
[12] V. Kaushal, M. Najafi, Comparative analysis of environmental and social costs of trenchless cured-in-place pipe renewal method with open-cut pipeline replacement for sanitary sewers, J. Pipel. Syst. Eng. Pract. 11 (4) (2020) 4020037, https://doi.org/10.1061/(ASCE)PS.1949-1204.0000480.
[13] J.C. Matthews, Large-diameter sewer rehabilitation using a fiber-reinforced cured-in-place pipe, Pract. Period. Struct. Des. Constr. 20 (2) (2015) 4014031, https://doi.org/10.1061/(ASCE)SC.1943-5576.0000231.
[14] J. Matthews, Sewer rehabilitation using an ultraviolet-cured GFR cured-in-place pipe, Pract. Period. Struct. Des. Constr. 20 (1) (2015) 4014021, https://doi.org/10.1061/(ASCE)SC.1943-5576.0000216.
[15] T.O. Adebola, I.D. Moore, N.A. Hoult, Use of optical fibers to investigate the performance of pressure pipe liners spanning across a ring fracture, Tunn. Undergr. Space Technol. 119 (2022) 104229, https://doi.org/10.1016/j.tust.2021.104229.
[16] M.J.P. Brown, I.D. Moore, A. Fam, Analysis of a cured-in-place pressure pipe liner spanning circular voids, Tunn. Undergr. Space Technol. 101 (2020) 103424, https://doi.org/10.1016/j.tust.2020.103424.
[17] K.J. Shou, C.C. Huang, Numerical analysis of straight and curved underground pipeline performance after rehabilitation by cured-in-place method, Undergr. Space. 5 (1) (2020) 30–42, https://doi.org/10.1016/j.undsp.2018.10.003.
[18] C. Argyrou, T.D. O'Rourke, H.E. Stewart, B.P. Wham, Large-scale fault rupture tests on pipelines reinforced with cured-in-place linings, J. Geotech. Geoenviron. Eng. 145 (3) (2019) 4019004, https://doi.org/10.1061/(ASCE)GT.1943-5606.0002018.
[19] H. Fang, K. Yang, B. Li, H. He, B. Xue, Parameter analysis of wall thickness of cured-in-place pipe linings for semistructured rehabilitation of concrete drainage pipe, Math. Probl. Eng. 2020 (2020) 1–16, https://doi.org/10.1155/2020/5271027.
[20] K. Yang, B. Xue, H. Fang, X. Du, B. Li, J. Chen, Mechanical sensitivity analysis of pipe-liner composite structure under multi-field coupling, Structures. 29 (2021) (2021) 484–493, https://doi.org/10.1016/j.istruc.2020.11.036.
[21] B. Li, H. Fang, K. Zhai, K. Yang, X. Zhang, Y. Wang, Mechanical behavior of concrete pipes with erosion voids and the effectiveness evaluation of the polyurethane grouting, Tunn. Undergr. Space Technol. 129 (2022) (2022) 104672, https://doi.org/10.1016/j.tust.2022.104672.
[22] R. Wang, F.M. Wang, J.G. Xu, Y.H. Zhong, S.K. Li, Full-scale experimental study of the dynamic performance of buried drainage pipes under polymer grouting trenchless rehabilitation, Ocean Eng. 181 (2019) (2019) 121–133, https://doi.org/10.1016/j.oceaneng.2019.04.009.
[23] C.F. Ihle, A. Tamburrino, Uncertainties in key transport variables in homogeneous slurry flows in pipelines, Miner. Eng. 32 (2012) (2012) 54–59, https://doi.org/10.1016/j.mineng.2012.03.002.

[24] W. Zhou, Reliability evaluation of corroding pipelines considering multiple failure modes and time-dependent internal pressure, J. Infrastruct. Syst. 17 (4) (2011) 216–224, https://doi.org/10.1061/(ASCE)IS.1943-555X.0000063.
[25] H. Fang, B. Li, F. Wang, Y. Wang, C. Cui, The mechanical behaviour of drainage pipeline under traffic load before and after polymer grouting trenchless repairing, Tunn. Undergr. Space Technol. 74 (2018) (2018) 185–194, https://doi.org/10.1016/j.tust.2018.01.018.
[26] B. Li, F. Wang, H. Fang, K. Yang, X. Zhang, Y. Ji, Experimental and numerical study on polymer grouting pretreatment technology in void and corroded concrete pipes, Tunn. Undergr. Space Technol. 113 (2021) (2021) 103842, https://doi.org/10.1016/j.tust.2021.103842.
[27] H. Shimada, Y. Chen, K. Araki, T. Sasaoka, K. Matsui, Experimental and numerical investigations of ground deformation using chemical grouting for pipeline foundation, Geotech. Geol. Eng. 30 (2) (2012) 289–297, https://doi.org/10.1007/s10706-011-9467-0.
[28] Code for construction and acceptance of water and sewerage pipeline works, in: GB 50268-2008, China Architecture & Building Press, Beijing, 2008.
[29] M. Oualit, R. Jauberthie, F. Rendell, Y. Melinge, M.T. Abadlia, External corrosion to concrete sewers: a case study, Urban Water J. 9 (6) (2012) 429–434, https://doi.org/10.1080/1573062X.2012.668916.
[30] Astm, Standard Practice for Rehabilitation of Existing Pipelines and Conduits by the Inversion and Curing of a Resin-Impregnated Tube, Astm (2021).
[31] Concrete and reinforced concrete sewer pipes, in: GB/T 11836-2009, Standards Press of China, Beijing, 2009.
[32] J. Lee, G.L. Fenves, Plastic-damage model for cyclic loading of concrete structures, J. Eng. Mech. 124 (8) (1998) 892–900, https://doi.org/10.1061/(ASCE)0733-9399(1998)124:8(892).
[33] L. Quan-Lin, Y. Min, Analytical model and parameters determination of interaction between buried pipe and soil, Yantu Lixue/Rock Soil Mech. 25 (5) (2004) 728–731.
[34] M. Xu, D. Shen, B. Rakitin, The longitudinal response of buried large-diameter reinforced concrete pipeline with gasketed bell-and-spigot joints subjected to traffic loading, Tunn. Undergr. Space Technol. 64 (2017) 117–132, https://doi.org/10.1016/j.tust.2016.12.020.
[35] H. Lu, Z. Xu, T. Iseley, J.C. Matthews, Novel data-driven framework for predicting residual strength of corroded pipelines, J. Pipel. Syst. Eng. Pract. 12 (4) (2021) 4021045, https://doi.org/10.1061/(ASCE)PS.1949-1204.0000587.
[36] J. Buco, F. Emeriault, R. Kastner, Full-scale experimental determination of concrete pipe joint behavior and its modeling, J. Infrastruct. Syst. 14 (3) (2008) 230–240, https://doi.org/10.1061/(ASCE)1076-0342(2008)14:3(230).
[37] M. Zhou, I.D. Moore, H. Lan, Experimental study on gasketed bell-and-spigot joint behaviour of lined-corrugated HDPE pipe subjected to normal fault., Géotechnique. 73 (9) (2023) 798-810, doi:10.1680/jgeot.21.00196.
[38] J. Shi, Y. Wang, C.W.W. Ng, Numerical parametric study of tunneling-induced joint rotation angle in jointed pipelines, Can. Geotech. J. 53 (12) (2016) 2058–2071, https://doi.org/10.1139/cgj-2015-0496.
[39] B. Rakitin, M. Xu, Centrifuge testing to simulate buried reinforced concrete pipe joints subjected to traffic loading, Can. Geotech. J. 52 (11) (2015) 1762–1774, https://doi.org/10.1139/cgj-2014-0483.
[40] K. Yang, H. Fang, X. Zhang, B. Li, Q. Hu, Investigation of mechanical properties of corroded concrete pipes after cured-in-place-pipe (CIPP) rehabilitation under multi-field coupling, Tunn. Undergr. Space Technol. 128 (2022) 104656, https://doi.org/10.1016/j.tust.2022.104656.
[41] B.C. Mondal, A.S. Dhar, Burst pressure of corroded pipelines considering combined axial forces and bending moments, Eng. Struct. 186 (2019) 43–51, https://doi.org/10.1016/j.engstruct.2019.02.010.
[42] K.J. Zhai, H.Y. Fang, M. Yang, M.M. Sun, X.J. Zhang, X.H. Zhao, B.H. Xue, J.W. Lei, X.P. Yao, The impacts of CFRP widths and thicknesses on the strengthening of PCCP, Structures. 56 (2023), https://doi.org/10.1016/j.istruc.2023.07.046.
[43] M. Fisz, Probability Theory and Mathematical Statistics, Probability theory and mathematical statistics, 1999.